ADVANCED MATERIALS

diameters of Pd nanowires without chemical contaminations and deformations are obtained after removal of the silica matrix using aqueous HF. Our study indicates that mesoporous silicas such as C_{16}MCM-41, C_{22}MCM-41, and SBA-15 can act as good templates for the synthesis of Pd nanowires. Moreover, a significantly depressed melting point of the Pd nanowires is observed around 300 °C. To the best of our knowledge, this is the first report on the synthesis and thermal behavior of Pd nanowires of less than 10 nm diameter.

Along with our matrix-assisted process, in particular, our low-temperature CVI approach is attractive because it can be carried out under conditions mild enough to avoid any disruption of both the desired material and the template structure. The combined matrix-assisted and CVI process can be extended not only to other sizes of nanowires but also to multidimensional structures using appropriate host architectures.

Received: September 25, 2000
Final version: November 15, 2000

[1] a) A. P. Alivisatos, *Science* **1996,** *271,* 933. b) D. L. Leslie-Pelecky, R. D. Rieke, *Chem. Mater.* **1996**, *8*, 1770. c) G. Schmid, *Chem. Rev.* **1992**, *92*, 1709. d) C. B. Murray, D. J. Norris, M. G. Bawendi, *J. Am. Chem. Soc.* **1993**, *115*, 8706.

[2] a) A. M. Morales, C. M. Lieber, *Science* **1998**, *279*, 208. b) X. Duan, C. M. Lieber, *Adv. Mater.* **2000**, *12*, 298.

[3] a) J. Sloan, D. M. Wright, H.-G. Woo, S. Bailey, G. Brown, A. P. E. York, K. S. Coleman, J. L. Hutchison, M. L. H. Green, *Chem. Commun.* **1999**, 699. b) A. Govindaraj, B. C. Satishkumar, M. Nath, C. N. R. Rao, *Chem. Mater.* **2000**, *12*, 202.

[4] a)C. R. Martin, *Chem. Mater.* **1996**, *8*, 1739. b) C. Schönenberger, B. M. I. Van der Zande, L. G. J. Fokkink, M. Henny, C. Schmid, M. Krüger, A. Bachtold, R. Huber, H. Birk, U. Staufer, *J. Phys. Chem. B* **1997**, *101*, 5497. c) L. Sun, P. C. Searson, C. L. Chien, *Appl. Phys. Lett.* **1999**, *74*, 2803. d) S. Shingubara, O. Okino, Y. Sayama, H. Sakaue, T. Takahagi, *Solid-State Electronics* **1999**, *43*, 1143. e) S. A. Sapp, B. B. Lakshmi, C. R. Martin, *Adv. Mater.* **1999**, *11*, 402.

[5] a) A. Sugawara, T. Coyle, G. G. Hembree, M. R. Scheinfein, *Appl. Phys. Lett.* **1997**, *70*, 1043. b) A. M. van de Craats, J. M. Warmam, K. Müllen, Y. Geerts, J. D. Brand, *Adv. Mater.* **1998**, *10*, 36. c) A. Kida, H. Kajiyama, S. Heike, T. Hashizume, K. Koike, *Appl. Phys. Lett.* **1999**, *75*, 540. d) B. R. Matrin, D. J. Dermody, B. D. Reiss, M. Fang, L. A. Lyon, M. J. Natan, T. E. Mallouk, *Adv. Mater.* **1999**, *11*, 1021. e) S. Fullam, D. Cottel, H. Rensmo, D. Fitzmaurice, *Adv. Mater.* **2000**, *12*, 1430.

[6] a) S.-W. Kim, S. U. Son, S. I. Lee, T. Hyeon, Y. K. Chung, *J. Am. Chem. Soc.* **2000**, *122*, 1550. b) C. P. Mehnert, D. W. Weaver, J. Y. Ying, *J. Am. Chem. Soc.* **1998**, *120*, 12 289. c) S. Suvanto, J. Hukkamäki, T. T. Pakkanen, T. A. Pakkanen, *Langmuir* **2000**, *16*, 4109.

[7] C. Wu, T. Bein, *Science* **1994**, *264*, 1757.

[8] a) Y. Plyuto, J. Berquier, C. Jacquiod, C. Ricolleau, *Chem. Commun.* **1999**, 1653. b) Y. J. Han, J. M. Kim, G. D. Stucky, *Chem. Mater.* **2000**, *12*, 2068. c) M. H. Huang, A. Choudrey, P. Yang, *Chem. Commun.* **2000**, 1063.

[9] a) G. D. Stucky, J. E. MacDougall, *Science* **1990**, *247*, 669. b) H. Winkler, A. Birkner, V. Hagen, I. Wolf, R. Schmechel, H. von Seggern, R. A. Fischer, *Adv. Mater.* **1999**, *11*, 1444. c) H. Parala, H. Winkler, M. Kolbe, A. Wohlfart, R. A. Fischer, R. Schmechel, H. von Seggern, *Adv. Mater.* **2000**, *12*, 1050.

[10] a) The templates of C_nMCM-41 (n = 16, 22) were prepared using alkyltrimethylammonium ($C_nH_{2n+1}(CH_3)_3N^+$; n = 12, 14), alkyltriethylammonium ($C_nH_{2n+1}(C_2H_5)_3N^+$; n = 22), or a mixture of alkyltrimethylammonium and alkyltriethylammonium surfactants of the same alkyl chain length (n = 16, 18, and 20). See: R. Ryoo, J. M. Kim, *J. Chem. Soc., Chem. Commum.* **1995**, 711. b) Mesoporous silica SBA-15 was synthesized by using triblock copolymer poly(ethylene oxide)–poly(propylene oxide)–poly(ethylene oxide) $EO_{20}PO_{70}EO_{20}$ surfactant in acidic conditions. See: D. Zhao, J. Feng, Q. Huo, N. Melosh, G. H. Fredrickson, B. F. Chmelka, G. D. Stucky, *Science* **1998**, *279*, 548.

[11] The $Pd(hfac)_2$ was synthesized by a reported method. A. R. Siedle, R. A. Newmark, A. A. Kruger, L. H. Pignolet, *Inorg. Chem.* **1981**, *20*, 3399. The $Pd(hfac)_2$ is known to absorb readily on silica surfaces by means of strong Lewis acid–base interaction between the Pd center and surface hydroxyl group and is very volatile at low temperature. See: A. R. Siedle, R. A. Newmark, *J. Am. Chem. Soc.* **1981**, *103*, 1240.

[12] a) The powder X-ray diffraction patterns were performed using a Rigaku Miniflex (0.5 kW) diffractometer with Cu Kα radiation (λ = 0.1545 nm) and samples were placed on a 33 mm diameter aluminum holder. b) EDAX and TEM images were carried out on the EM 912 Omega TEM operating at 120 kV accelerating voltage.

[13] B. Marler, U. Oberhagemann, S. Vortmann, H. Gies, *Microporous Mater.* **1996**, *6*, 375.

[14] G. E. Muilenberg, *Handbook of X-ray Photoelectron Spectroscopy*, Perkin–Elmer, Eden Prarie, MN **1978**. The XPS was measured with Omicron using an Mg Kα X-ray source. The EDAX revealed that the main composition of the wire-like objects was pure Pd.

[15] W. F. McClune, *JCPDS Powder Diffraction File*, International Center for Diffraction Data, Swarthmore, PA **1996**, JCPDS number 46-1043.

[16] a) A. N. Goldstein, C. M. Echer, A. P. Alivisatos, *Science* **1992**, *256*, 1425. b) A. P. Alivisatos, *J. Phys. Chem.* **1996**, *100*, 13 226.

[17] Z. Liu, Y. Sakamoto, T. Ohsuna, K. Hiraga, O. Terasaki, C. H. Ko, H. J. Shin, R. Ryoo, *Angew. Chem. Int. Ed.* **2000**, *39*, 3107.

Melting and Welding Semiconductor Nanowires in Nanotubes**

By *Yiying Wu* and *Peidong Yang**

One-dimensional nanostructures, such as nanowires and nanotubes, exhibit novel electronic and optical properties that are intrinsically associated with their low dimensionality and the quantum confinement effect. Nanowires of various compositions have recently been synthesized using chemical vapor deposition/transport and laser ablation methods.[1–5] To implement these nanoscale building blocks for nanoscale electronics,[6,7] their chemical and thermal stability have to be carefully considered because of their extremely fine sizes and high surface areas. To a certain extent, their chemical stability can be improved through proper surface passivation, for example, by creation of core–sheath structures.[8] This can, in principle, be achieved through nanowire formation by filling the hollow cavities of the nanotubes with elements or compounds[9–11] or direct synthesis of concentric nanocables.[12–14] It is expected that the existence of an extensive interface will inevitably alter the thermal stability of the nanowires. Herein, we report the interface-driven thermal instability of nanowires within nanotubes. Significant melting point depression, as well as large hysteresis during the melting–recrystallization cycle, were observed for semiconductor Ge nanowires encapsulated within carbon nanotubes. It is further demonstrated that it is possible to manipulate individual nanowires through proper thermal treatment.

Ge nanowires with diameters from 10–100 nm were synthesized via the vapor–liquid–solid mechanism using gold nano-

[*] Prof. P. Yang, Y. Wu
Department of Chemistry, University of California
Berkeley, CA 94720 (USA)
E-mail: pyang@cchem.berkeley.edu

[**] This work was supported in part by the Camille and Dreyfus Foundation, Research Corporation and start-up funds from the University of California, Berkeley. P.Y. thanks the 3M company for an untenured faculty award. P.Y. also thanks Dr. E. Stach and D. C. Nelson for help with the TEM studies. We thank the National Center for Electron Microscopy for the use of their facilities.

  0935-9648/01/0704-0520 $ 17.50+.50/0

clusters as catalysts in a sealed-tube chemical vapor transport system.[4] Before the high-temperature in-situ transmission electron microscopy (TEM) studies the Ge nanowires are coated with a thin layer of carbon sheath in order to confine the molten Ge and prevent the formation of liquid spheres at high temperature. This can readily be achieved by pyrolysis of organic molecules on the nanowire surface.[8] Figure 1 shows high-resolution TEM images of the Ge nanowires before and after carbon sheath coating. The as-prepared Ge nanowires are highly crystalline and show [111] growth direction without any oxide layer coating. After coating, the wires are protected by a thin layer of porous graphite sheath. The thickness of this carbon sheath is generally ~1–5 nm. The lattice fringes from the sheath indicate that the interlayer distance is about 0.34 nm, similar to the (002) spacing of turbostratic graphitic carbon. These carbon-sheathed nanowires were dispersed on SiO_x TEM grids and were subjected to a thermal cycle within the microscope. The carbon-sheathed Ge nanowires are ideal for this study since Ge and carbon do not react or form an alloy under those experimental conditions. To avoid the possible interference of the Au/Ge catalyst tip during the melting study, we chose wires whose tips had been cleaved off by prolonged ultrasonication. Energy-dispersive X-ray (EDX) spectroscopy was used to make sure there is negligible impurity doping in the Ge nanowires. The melting point (T_m) of the nanowires is identified as the point at which the electron diffraction pattern disappears. The real-time melting and recrystallization behavior of the nanowires was monitored in the bright-field mode.

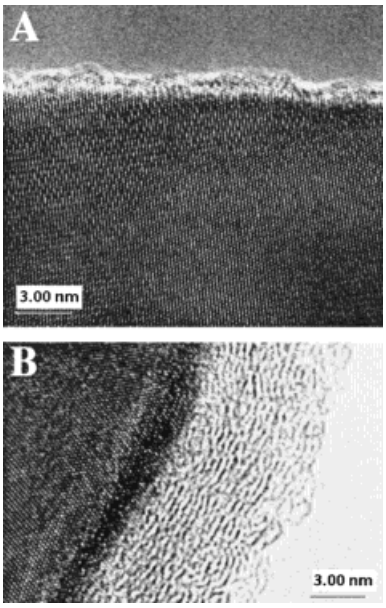

Fig. 1. High-resolution transmission electron microscopy images of as-prepared Ge nanowires (A), and carbon-sheathed Ge nanowires (B). Both nanowires have a [111] growth direction.

During the experiments, the sample stage was resistively heated in 10 °C steps, up to 10 °C beyond T_m, and cooled stepwise. The average heating and cooling rates range from 5 to 20 °C/min. Two important features during the thermal cycle were observed. First, there is a significant decrease of the melting point for the Ge nanowires with diameters of 10–100 nm. For example, a Ge nanowire with diameter of 55 nm and length of 1 μm starts melting at around 650 °C (the melting point for bulk Ge is 930 °C). Figure 2 shows the TEM image sequence during the melting of this Ge nanowire. Melting of these nanowires generally starts at the two ends of the wire, presumably because the melting point is the lowest where the particle curvature is the highest, i.e., at the tip of the wires. The molten liquid front moves towards the middle of the wires at a velocity of 3–20 nm/s (Fig. 2A–2E). The solid/liquid interface has a concave meniscus. At 848 °C, the whole wire melts and the molten Ge nanowire is confined within the carbon sheath (Fig. 2E). It was further found that, during the cooling process, the recrystallization of these molten Ge nanowires occurs at much lower temperatures than the initial melting temperature (for example, 558 °C for the 55 nm Ge wire, Fig. 2F). The molten nanowires generally recrystallize in less than one second. As a comparison, the melting process for these nanowires also dramatically differs from those for nanoparticles and nanorods, which generally involve surface melting.[15–17]

Figure 3A shows the melting–recrystallization hysteresis for three nanowires with different diameters and similar lengths. It was found that thinner wires melt and recrystallize at lower temperatures. The melting point depression for materials in confined geometry has been simulated with a confined 1D liquid model.[18–20] Within this model, the melting point decrease ΔT can be related to the radius (r) of the wires as follows:

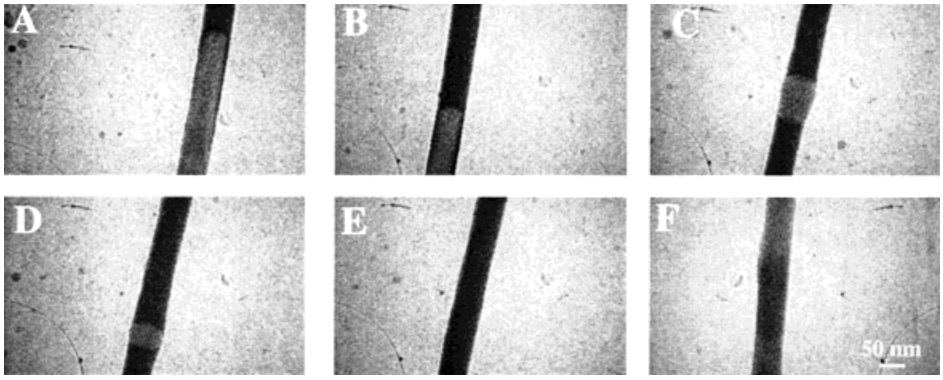

Fig. 2. The melting and recrystallization process for a 55 nm Ge nanowire. The carbon-sheathed nanowires are dispersed on a SiO_x TEM grid, and loaded onto a heating stage within a JEOL 200CX high-temperature microscope. Electron diffraction was used to distinguish the solid and molten states. The molten Ge does not have a diffraction contrast and appears dark in the image. The electron diffraction experiments were conducted such as to minimize spurious beam heating. The beam current was maintained at 10 μA above the dark current, well below fluxes commonly required to effect beam-induced transformations. The melting–recrystallization process was monitored with video camera in bright-field mode. A) 766 °C, B) 780 °C, C) 842 °C, D) 847 °C, E) 848 °C, and F) 558 °C.

  0935-9648/01/0704-0521 $ 17.50+.50/0

ADVANCED MATERIALS

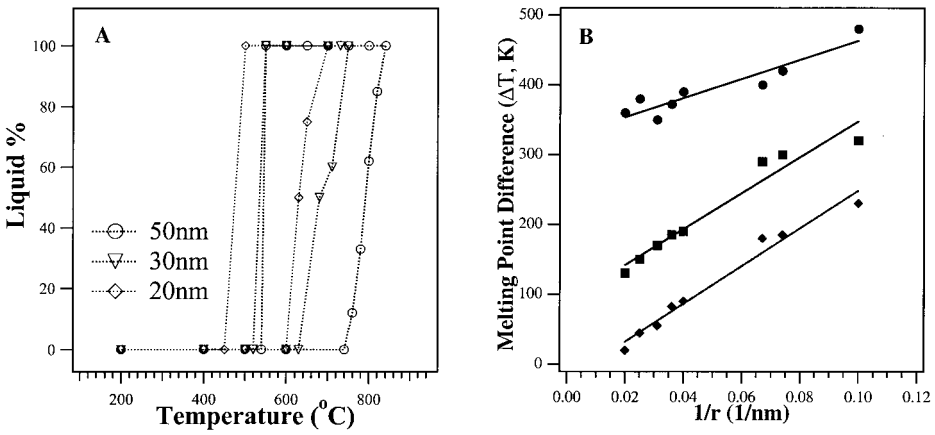

Fig. 3. A) The melting–recrystallization hysteresis curves observed for nanowires with diameters of 20 (◇), 30 (▽), and 50 nm (○). The wires chosen for this study generally had lengths of 0.8–1 μm. B) The melting point suppression (ΔT) is plotted against the inverse of the nanowire radius $1/r$. The suppression derived from the initial melting point (■); the suppression derived from the final melting temperature (◆); the suppression derived from the recrystallization temperature (●). The fitted lines are a guide to the eye.

$$\Delta T = 2\sigma\nu T_0/\Delta H_f r \quad (1)$$

where ΔH_f is the heat of fusion, T_0 the bulk melting point, ν the molar volume, and σ the difference between the solid/wall interfacial energy and the liquid/wall interfacial energy. Although the melting point suppression ΔT for the final melting of our nanowires approximately correlates with the inverse of the nanowire radius, this confined 1D liquid model is not able to accurately account for the large melting point suppression values that are generally observed to be 120–300 °C for the initial melting and 50–200 °C for final melting (Fig. 3B). Interestingly, we also found that the melting process is length dependent, with the final melting points approaching the bulk value as the nanowires get longer. We believe that the large melting–recrystallization hysteresis for these wires is due to the presence of a kinetic barrier for homogeneous/heterogeneous crystallization[21] within the nanotubes. This type of hysteresis has often been observed in the freezing/melting transition of materials confined in the conventional mesoscale channels, such as Vycor glass and sol–gel glasses. It should, however, be pointed out that the supercooling of ~300–400 °C for nanowires in nanotubes is significantly higher than the largest value observed for supercooling of the Ge system (230 °C for micrometer sized droplets).[22] The exact reason for this significant supercooling remains unclear at this stage and merits further investigation.[23]

Utilizing the low melting points of the nanowires encapsulated in nanotubes, we are able to manipulate individual nanowires, for example, in-situ cutting, interconnection, and welding. After the nanowires have been melted, it is observed that during the cooling process, if the carbon sheath at the tip is thin enough, the sheath ruptures and liquid Ge sprays out from the tube to form liquid droplet reservoirs at the ends of the wire. The molten Ge nanowires then break in the middle (a thermal cutting process). At temperatures between 450 and 600 °C, the remaining Ge liquid core can be quenched and recrystallized. Figure 4 shows the resulting two nanowires separated by a vacuum gap after the thermal cutting process. The recrystallized wires maintain the [111] orientation as shown in the inset.

Interestingly, It is further possible to connect two nanowires into one single-crystalline nanowire. Figure 5A–F shows such a process, where we started with two single-crystalline nanowires within a nanotube (Fig. 5A). When the temperature increases, the two nanowires melt, the liquid fronts move towards each other, and eventually merge to form a single wire after recrystallization. This process apparently utilizes the local Ge vapor as material supply to fill the gap.

Besides simple cutting and linking, we are also able to carry out localized welding between two crossed nanowires at relatively low temperatures. Figure 6 shows two cross junctions formed by heating two crossed nanowires in the microscope. This type of localized welding is possible due to the porous nature of the carbon sheath, especially for those wires with thin coating (~1 nm), which allows the molten Ge to exchange at the contact point. The liquid eventually fuses together to form a homojunction. These junctions generally have much sharper interfaces compared to those junctions formed by sequential vapor-phase growth or by the direct reaction of nanotubes with bulk solids.[12,24] This approach utilizes the localized nanoscale reaction and should readily be applicable to the creation of many other heterojunctions where semiconductor nanowires and carbon nanotubes are used as building blocks.

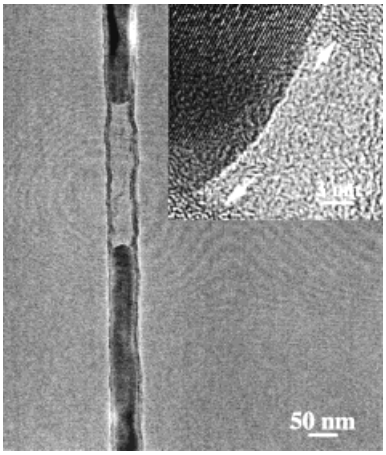

Fig. 4. TEM image of two Ge nanowires separated by a vacuum gap, created by the thermal cutting process. The inset shows a high-resolution TEM image at the wire–tube interface. The (111) lattice fringe of the Ge nanowire can clearly be seen.

  0935-9648/01/0704-0522 $ 17.50+.50/0

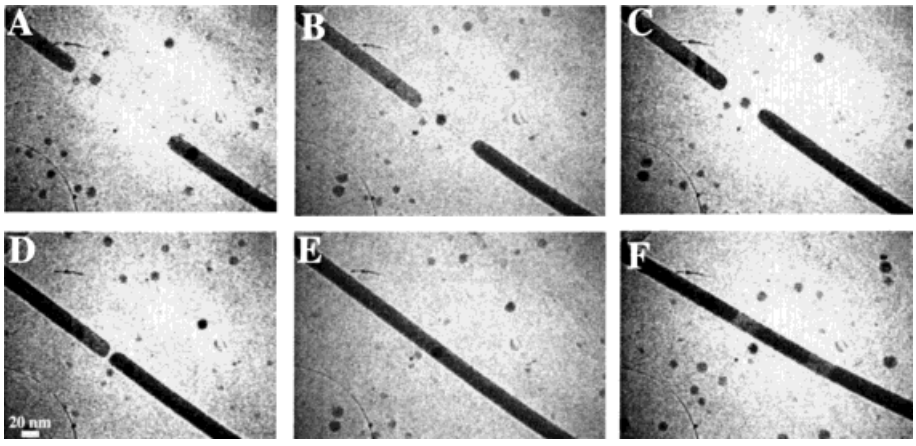

Fig. 5. The TEM image sequence of linking two nanowires within a nanotube. The temperature is kept at 850 °C during the operation (A–E). After interconnection, the wire is quenched and recrystallized at 540 °C (F).

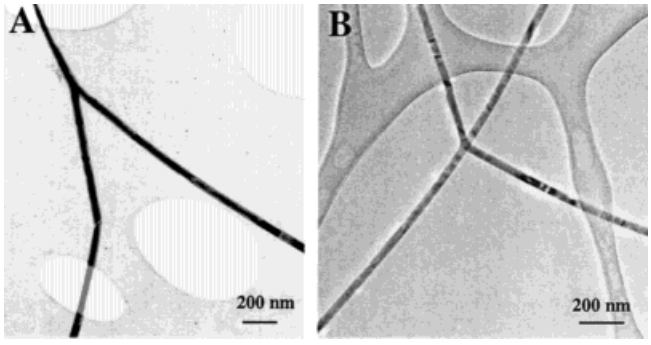

Fig. 6. Two nanowire junctions formed through local welding between two crossed nanowires. The nanoscale welding occurs at 800–900 °C, depending on the diameter of the nanowires, and the junctions are quenched and recrystallized after the welding.

The marked reduction in melting temperature for the reported nanowires in nanotubes has several important implications. Firstly, the optimum annealing temperature for the preparation of high-quality, defect-free nanowires can be expected to be a small fraction of the bulk annealing temperature. It is thus possible to conduct nanowire zone-refining at modest temperatures with the current, simple configurations. Secondly, the capability of cutting, linking, and welding nanowires at relatively modest temperatures may provide a new approach to integrating these 1D nanostructures into functional devices and circuitry. Finally, as the length of the wires is reduced to nanometer scales, the chemical and thermal stability of new devices may be limited; this should also be considered during the implementation of these wires in nanoscale electronics.

Received: November 17, 2000
Final version: January 22, 2001

[1] A. M. Morales, C. M. Lieber, *Science* **1998**, *279*, 208.
[2] Y. F. Zhang, Y. H. Tang, N. Wang, D. P. Yu, C. S. Lee, I. Bello, S. T. Lee, *Appl. Phys. Lett*. **1998**, *72*, 1835.
[3] J. Hu, T. W. Odom, C. M. Lieber, *Acc. Chem. Res.* **1999**, *32*, 435.
[4] Y. Wu, P. Yang, *Chem. Mater*. **2000**, *12*, 605.
[5] X. Duan, C. M. Lieber, *Adv. Mater*. **2000**, *12*, 298.
[6] M. S. Fuhrer, J. Nygard, L. Shih, M. Forero, Y. G. Yoon, M. S. C. Mazzoni, H. J. Choi, J. Ihm, S. G. Louie, A. Zettl, P. L. McEuen, *Science* **2000**, *288*, 494.
[7] T. Rueckes, K. Kim, E. Joselevich, G. Y. Tseng, C. L. Cheung, C. M. Lieber, *Science* **2000**, *289*, 94.
[8] Y. Wu, P. Yang, *Appl. Phys. Lett*. **2000**, *77*, 43.
[9] W. K. Hsu, Y. Q. Zhu, H. W. Kroto, D. R. M. Walton, R. Kamalakaran, M. Terrones, *Chem. Phys. Lett*. **1998**, *284*, 177.
[10] S. C. Tsang, Y. K. Chen, P. J. F. Harris, M. L. H. Green, *Nature* **1994**, *372*, 159.
[11] A. Loiseau, H. Pascard, *Chem. Phys. Lett*. **1996**, *256*, 246.
[12] Y. Zhang, T. Ichihashi, E. Landree, F. Nihey, S. Iijima, *Science* **1999**, *285*, 1719.
[13] Y. Zhang, K. Suenaga, C. Colliex, S. Iijima, *Science* **1998**, *281*, 973.
[14] K. Suenaga, C. Colliex, N. Demoncy, A. Loiseau, H. Pascard, F. Willaime, *Science* **1997**, *278*, 653.
[15] A. N. Goldstein, C. M. Echer, A. M. Alivisatos, *Science* **1992**, *256*, 1425.
[16] Z. L. Wang, J. M. Petroski, T. C. Green, M. A. El-Sayed, *J. Phys. Chem. B* **1998**, *102*, 6145.
[17] S. Link, Z. L. Wang, M. A. El-Sayed, *J. Phys. Chem. B* **2000**, *104*, 7867.
[18] D. D. Awschalom, J. Warnock, *Phys. Rev. B* **1987**, *35*, 6779.
[19] E. V. Charnaya, C. Tien, K. J. Lin, Y. A. Kumzerov, *Phys. Rev. B* **1998**, *58*, 11 089.
[20] K. M. Unruh, T. E. Huber, C. A. Huber, *Phys. Rev. B* **1993**, *48*, 9021.
[21] D. Turnbull, *J. Appl. Phys*. **1950**, *21*, 1022.
[22] D. Turnbull, R. E. Cech, *J. Appl. Phys*. **1950**, *21*, 804.
[23] Nanotube size-dependent melting of single crystals in carbon nanotubes was studied theoretically by Q. Jiang, N. Aya, F. G. Shi, *Appl. Phys. A* **1997**, *64*, 627. The proposed model, however, also underestimates the supercooling, which proves to be inconsistent with the experimental data. For example, 80 °C of supercooling is estimated for a 20 nm Ge nanowire, which is significantly smaller than our observed value.
[24] J. Hu, M. Ouyang, P. Yang, C. M. Lieber, *Nature* **1999**, *399*, 48.

  0935-9648/01/0704-0523 $ 17.50+.50/0